CHAPTER VI

EFFECT OF SiO_2 PORE SIZE ON PARTIAL HYDROGENATION OF RAPESEED OIL-DERIVED FAMES

(Published in Applied Catalysis A: General, 441–442 (2012) 72–78)

6.1 Abstract

Palladium (Pd) supported on different SiO_2 pore sizes: Q3, Q10, Q30, and Q50 with pore diameters of 3, 5, 30, and 50 nm, respectively, were studied for the partial hydrogenation of rapeseed oil-derived fatty acid methyl esters (FAMEs). The supports and catalysts were characterized by BET, NH_3-adsorption, and CO-chemisorption technique. Highest turn over frequency (TOF) was found for Pd/Q30, while Pd/Q3 exhibited the lowest TOF. The reaction rate constants for each hydrogenation step, consequently from C18:3 to C18:2, C18:1, and C18:0, i.e., k_1, k_2, and k_3, respectively, were determined by POLYMATH Professional 6.2 and could explain the effect of SiO_2 pore size on pore diffusion of FAMEs reactant and contact probability between reactant molecules and active sites. Moreover, pore size of the SiO_2 support also affected on selectivity towards *trans*-monounsaturated FAME. The Pd/Q3 catalyst presented the lowest *trans*-monounsaturated FAME selectivity due to its smallest pore size and acidic properties. In addition, it was found that 0.5 h of hydrogenation time using Pd/Q10, Pd/Q30, and Pd/Q50 could improve the oxidative stability to > 10 h.

Keywords: partial hydrogenation; Pd/SiO_2; pore size; biodiesel; oxidative stability

6.2 Introduction

Biodiesel or fatty acid methyl ester (FAME) is known to be an alternative for petroleum-based diesel. Advantages of biodiesel are: renewability, biodegradability, higher flash point, higher cetane number, reduction of exhaust emissions, miscibility with petroleum-based diesel, and its ability to be produced domestically [1–3]. However, its fuel properties correspond to natural characteristics of starting oil or fat [4]. Structural features that influence the fuel properties of biodiesel are chain length, degree of saturation, and branching of the chain [5]. Degree of saturation of fatty acid has strong effects on the quality of biodiesel especially oxidative stability and cold flow properties. Biodiesel produced from vegetable oil that contains higher unsaturated fatty acid composition exhibits lower oxidative stability. In contrast, the higher the saturated fatty acid composition, the worse cold flow properties become. Therefore, partial hydrogenation of polyunsaturated FAMEs to monounsaturated ones is a promising solution to these problems.

The catalysts used in commercial hydrogenation of triglycerides are usually Ni catalysts supported on silica or alumina, and mostly used in the slurry phases. These Ni catalysts are cheaper than noble metal catalysts, but more severe hydrogenation pressure is required for the former compared with the latter ones [6–7]. In this respect, noble metal catalysts such as Pd seem to be the most promising [8]. Supported Pd catalysts have been widely employed as catalysts for hydrogenation reaction [9–10]. Materials usually used as a catalyst support are: carbon [11–13], silica [14–15], alumina [16–17], and zeolite [18–19]. Due to the difference in nature and structure of each support, the type of support is believed to affect catalytic activity and selectivity of the catalyst. Moreover, the same support with different pore size also affects the rate and selectivity of the reaction [7]. The effect of pore size of the support on the catalytic activity has been investigated in liquid phase hydrogenation of many reactants. For example; hydrogenation of 1-hexene [20], cinnamaldehyde to cinnamyl alcohol [21], and methyl linoleate [12] have been studied.

In this study, mesoporous SiO_2 has received considerable attention as a support for Pd catalyst because of its uniform pore size with a variety of pore diameters in a range from 3 nm to 50 nm, which is a good representative for a study of pore size effect of the support. Therefore, we focused on the improvement of oxidative stability of rapeseed oil-derived biodiesel by partial hydrogenation over Pd/SiO_2 catalysts. The effect of pore size of the SiO_2 support was investigated in terms of catalytic activity, turn over frequency (TOF), selectivity, and fuel properties. In addition, kinetic analysis was also studied by determining the reaction rate constant of each hydrogenation step, from C18:3 to C18:2, C18:1, and C18:0, consequently (k_1, k_2, and k_3, respectively). This kinetic analysis demonstrated the effect of SiO_2 pore size on pore diffusion of FAMEs reactant very well.

6.3 Experimental

6.3.1 Catalyst Preparation

Four types of commercial silica with an average pore diameter of 3 nm (SiO_2-Q3), 10 nm (SiO_2-Q10), 30 nm (SiO_2-Q30), and 50 nm (SiO_2-Q50) purchased from Fuji Silysia Chemical Company Ltd., were used as supports. Pd on SiO_2 catalysts were prepared by incipient wetness impregnation with an aqueous solution containing appropriate amounts of $Pd(NH_3)_4.Cl_2$. The total amount of Pd loading was 1 wt.%. After impregnation, the catalyst was dried by a rotary evaporator at room temperature for 2 h, then at 60°C for 2 h, and finally by a vacuum pump at 60°C for 2 h. After that, it was calcined under an oxygen stream at 300°C with a heating rate of 0.5°C/min and 1 L/min of oxygen flow rate. Finally, the catalyst was reduced at 300°C for 2 h with a heating rate of 5°C/min and 100 ml/min hydrogen flow rate before use in the partial hydrogenation reaction. The prepared Pd supported on SiO_2-Q3, SiO_2-Q10, SiO_2-Q30, and SiO_2-Q50 catalysts can be notified as Pd/Q3, Pd/Q10, Pd/Q30, and Pd/Q50, respectively.

6.3.2 Catalyst Characterization

The specific surface area, pore volume, and pore size distribution of the support were determined by N_2 physisorption using a Quantachrome Autosorb-1 MP surface area analyzer. Before analyzing, the sample was heated in a vacuum atmosphere at 250°C overnight to eliminate volatile species that had adsorbed on the surface.

Moreover, acidity of the SiO_2 support was investigated by the NH_3-adsorption technique using an NH_3 calorimeter (CSA-450G) manufactured by Tokyo Riko Co., Ltd. The sample was evacuated at 300°C for 1 h and cooled down to 50°C to measure the heat of adsorption of NH_3 on the acid sites.

Pd dispersion of the prepared catalysts was determined by pulse chemisorption of 10.1% CO/He, using Temperature-Programmed Desorption/Oxidation/Reduction (TPD/R/O) Ohkura R6015. Prior to measurements, the calcined sample was pretreated with hydrogen at 300°C for 1 h and followed by purging with helium at the same temperature for 10 min. The Pd dispersion was measured at 50°C and calculated by assuming a stoichiometry of CO:Pd = 1:1.

6.3.3 Transesterification of Rapeseed Oil

Fatty acid methyl esters (FAMEs) of rapeseed oil were prepared by a typical transesterification reaction catalyzed by potassium hydroxide (KOH). The reaction took place in a 2 L three-necked round-bottomed flask, equipped with a stirrer and a condenser. The amount of catalyst used was 1 wt.% compared to the starting rapeseed oil with 9:1 methanol to oil molar ratio. KOH was dissolved in methanol and added into the rapeseed oil. The mixture was stirred at 60°C for 2 h and cooled down. A phase separation was followed; the lower glycerine phase was removed. The upper phase was washed with 60°C distilled water several times to remove remaining KOH, methanol, and possible soap. Finally, it was dried by a rotary evaporator at 60°C, to remove remaining washed water. The FAME composition of the rapeseed biodiesel fuel (BDF) was determined by gas chromatography (GC).

6.3.4 Partial Hydrogenation of Polyunsaturated FAMEs

The partial hydrogenation reaction was carried out in a 388 ml stainless steel semi-batch reactor at a temperature and hydrogen partial pressure of 80°C and 0.3 MPa, respectively. The stirring rate was maintained at 1000 rpm and the flow rate of hydrogen gas was 200 Nml/min. The reactor was charged with approximately 180 ml of BDF feed and 0.3 g of Pd/SiO2 catalyst under a flow of Ar. The reactor was connected to the reaction line and the system was purged with nitrogen. The reaction proceeded under the desired conditions. Finally, the liquid products were collected every 30 min. The total reaction time was 3 h.

FAME composition in the biodiesel before and after the partial hydrogenation reaction was determined by using a Hewlett Packard gas chromatograph 6890N equipped with a flame ionization detector (GC-FID). An HP-88 (100 m x 250 μm x 0.2 μm) capillary column was used. Samples of 1 μl were injected under the following conditions: the carrier gas was helium with a flow rate of 2.4 ml/min, an injector temperature was 200°C with a split ratio of 75:1, and a detector temperature was 230°C. The sample was injected at an oven temperature of 155°C. After an isothermal period of 20 min, the GC oven was heated to 230°C at a rate of 2°C/min and held for 2.5 min with a total running time of 60 min. The FAME composition was identified by reference to the retention time.

The activity of the catalysts was studied in terms of TOF, which is the amount of reactant reacted per surface area of active site per time. Here, TOF was calculated as shown in Equation 6.1.

$$\text{TOF} = \frac{\text{Mole of FAMEs converted or formed per time}}{\text{Mole of Pd metal exposed on the surface}} \qquad (6.1)$$

whereas; the mole of Pd metal exposed on the surface was determined from Pd dispersion.

Oxidative stability is one of the major issues indicating the content of polyunsaturated FAMEs. The oxidative stability of hydrogenated biodiesel was tested by a Metrohm 743 Rancimat. The sample was aged at 110°C under a constant air stream with flow rate of 10 L/h. The oxidative stability corresponds to the period

of time before FAMEs are degraded to such an extent that the formation of volatile acids can be recorded through an increase in conductivity. This procedure was developed according to EN 14112 [22].

Furthermore, cold flow properties of biodiesel before and after partial hydrogenation including cloud point and pour point were investigated by using a Tanaka mini pour/cloud point tester Series MCP-102 that was developed according to ASTM D6749.

6.4 Results and Discussion

6.4.1 Support and Catalyst Characterization

The characteristics of the SiO_2 supports and Pd/SiO_2 catalysts were obtained using a BET-surface area analyzer and NH_3-adsorption, and CO-chemisorption, respectively.

Surface area and average pore diameter of SiO_2 supports were shown in Table 6.1. Figure 6.1 shows NH_3 heat of adsorption versus amount of NH_3 adsorbed of the SiO_2 supports analyzed by NH_3-chemisorption. As shown in Figure 6.1, SiO_2-Q3 exhibited weak acidic property (heat of adsorption 70–90 kJ/mol), whereas Q10 showed some weak acidic property. In contrast, Q30 and Q50 did not present any acidic properties. The acidic properties of SiO_2 support depend on the preparation condition. Dispersion of Pd is also an important characteristic that tells how well Pd metals disperse on the surface of the catalyst. The dispersion of Pd is displayed in Table 6.1. It is noticed that Pd dispersion did not follow the same trend as the surface area of the support, but higher Pd agglomeration was found in lower surface area SiO_2. However, the activity of the catalysts could be determined from the TOF, not directly from Pd dispersion.

Table 6.1 Physical properties of SiO_2-Q3, Q10, Q30, and Q50 used as a support in this study.

	Q3	Q10	Q30	Q50
Surface area (m^2/g)	700.8	281.1	112.1	69.2
Average pore diameter (nm)	2.6	16.4	45.3	68.3
Pd dispersion (%)	48.3	30.3	6.6	11.7

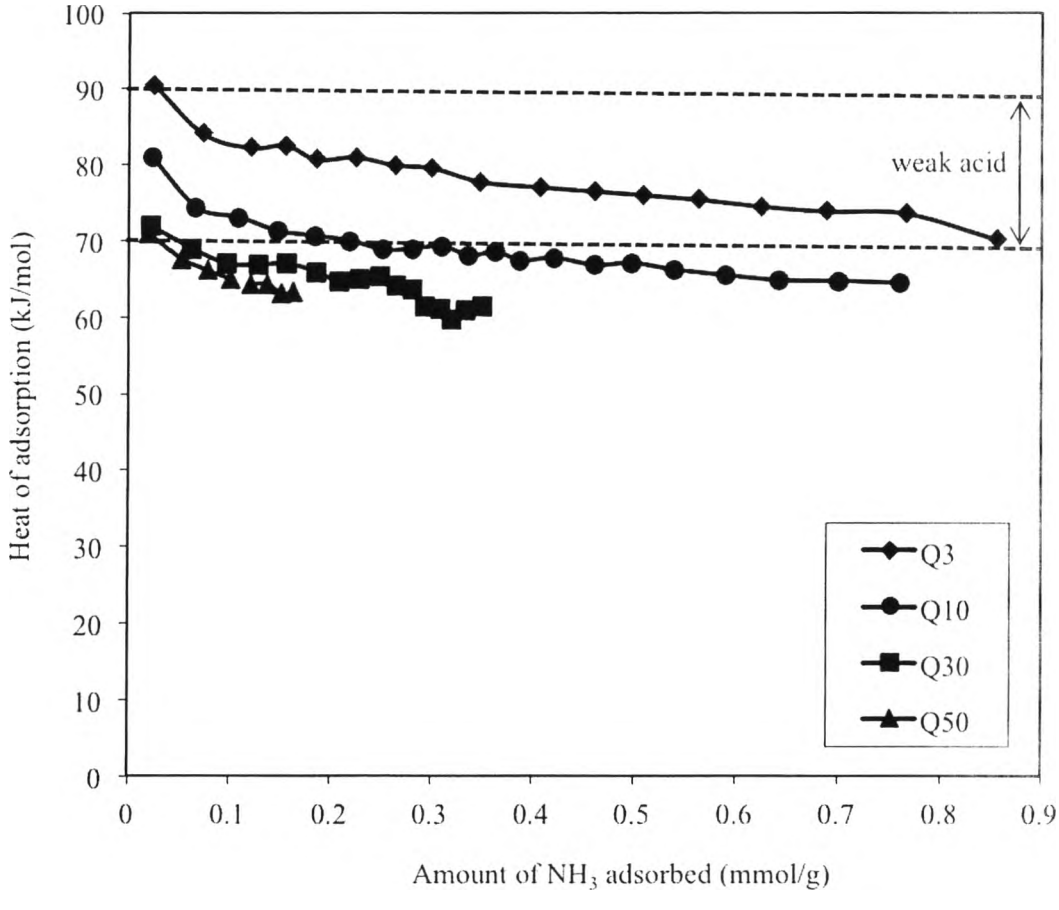

Figure 6.1 NH_3 heat of adsorption versus amount of NH_3 adsorbed of SiO_2 supports analyzed by NH_3-adsorption.

6.4.2 Partial Hydrogenation of Polyunsaturated FAMEs

In order to investigate the effect of pore size of SiO_2 support, partial hydrogenation of rapeseed BDF was operated and controlled at a condition of 80°C, 0.3 MPa, 200 Nml/min hydrogen flow rate, 1000 rpm stirring rate, and 0.2 wt.% of catalyst compared to the BDF.

Figure 6.2(A) and (B) show FAME composition as a function of reaction time using Pd/Q30. It showed that the longer the reaction time, the higher the conversion of polyunsaturated FAMEs. As shown in Figure 6.2(A), triunsaturated and diunsaturated FAMEs are gradually hydrogenated at the beginning of reaction with a gradual increase of monounsaturated and saturated FAMEs. At 0.6 h of reaction, triunsaturated FAMEs are fully hydrogenated. After that, at 1 h of reaction, monounsaturated FAMEs gradually decrease with a linearly increase of saturated FAMEs. This suggests that this Pd/SiO_2 catalyst meets the criteria in the partial hydrogenation point of view, which shows the behavior of consecutive reactions from tri-, di-, and monounsaturated FAMEs to saturated FAMEs.

Another interesting observation is an increase of *trans*-monounsaturated FAME composition with the reaction time as presented in Figure 6.2(B). This indicates that some of the unreacted *cis*-monounsaturated FAMEs are transformed into *trans*-configurations under this pressure and temperature [13]. As shown in Table 6.2, only *cis*-isomers are presented in natural BDF and they are more favorable monounsaturated derivatives due to better cold flow properties when compared with the *trans*-isomers [3]. The formation of *trans*-isomers during hydrogenation is consistent with the work done by Pérez-Cadenas and co-workers [23]. They found that hydrogenation and *cis-trans* isomerization of the C=C bonds simultaneously take place during the hydrogenation of vegetable oil or FAMEs.

The FAME composition and some fuel properties of rapeseed biodiesel and hydrogenated biodiesel product after 1 h of reaction using Pd/Q30 are reported in Table 6.2. It apparently shows that partial hydrogenation can improve the oxidative stability of biodiesel from 1.89 h to 38.98 h, which meets the Thai Standard (requires $\geq$ 10 h of oxidative stability) even without the addition of any antioxidants. However, the hydrogenated biodiesel exhibited a poor pour point and cloud point, which exposes a weakness in the cold flow properties of hydrogenated biodiesel.

However, this problem can be minimized by blending with petroleum diesel in a proper ratio [24]. Of course, the optimization of hydrogenation degree, i.e., compromising between oxidative stability and cold flow properties are now under investigation.

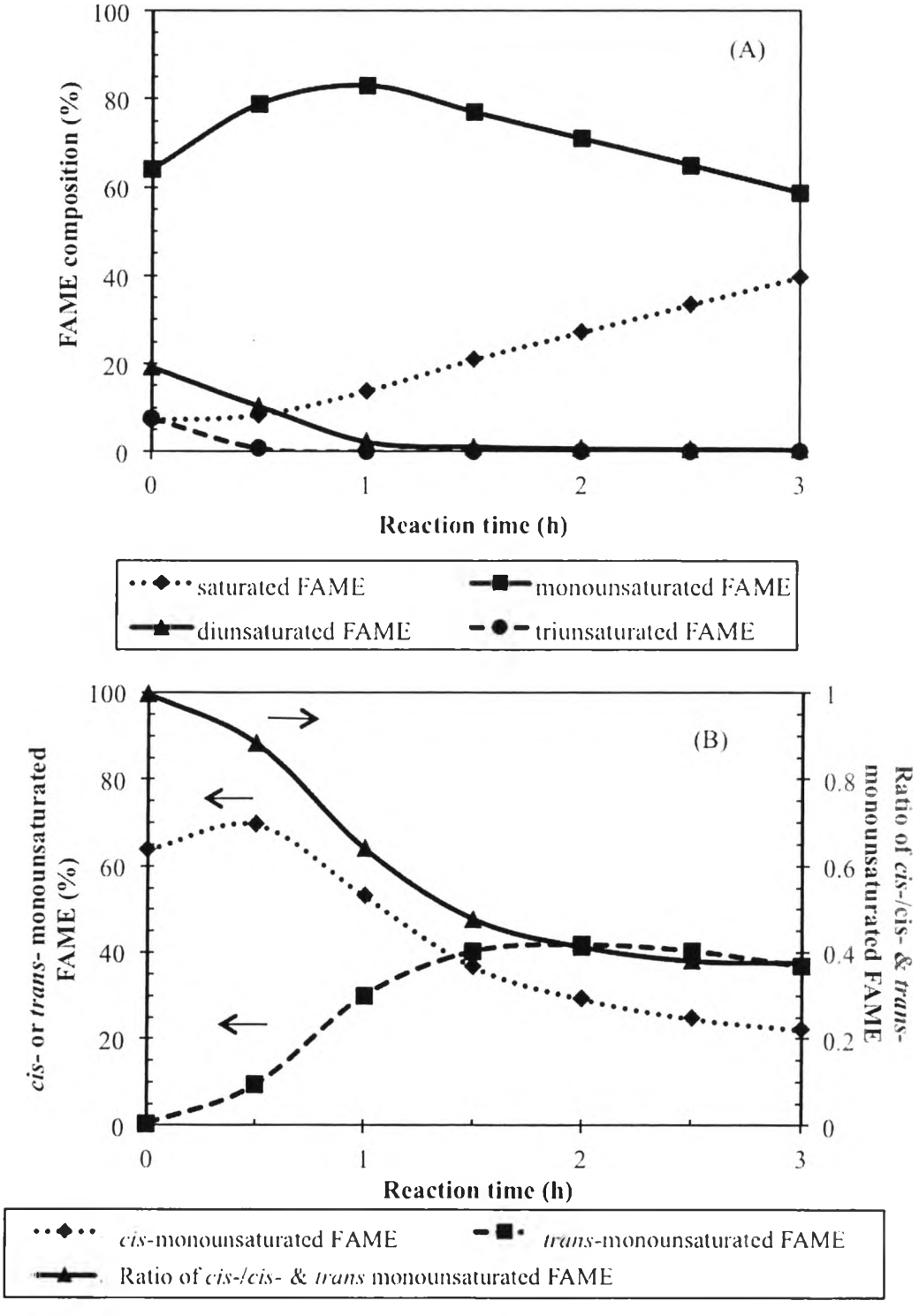

Figure 6.2 Overall FAME composition, (A) and *cis*- or *trans*-monounsaturated FAME composition, (B) as a function of reaction time using 1 wt.% Pd/Q30 (Reaction conditions: 0.3 g catalyst, 180 ml oil, 80°C, 0.3 MPa, 200 Nml/min hydrogen flow rate, and 1000 rpm stirring rate).

Table 6.2 FAMEs composition and some fuel properties of rapeseed BDF and hydrogenated BDF after 1 h of reaction using Pd/Q30.

FAME composition (%)	Rapeseed BDF	Hydrogenated BDF after 1 h
Saturated FAME	7.14	13.89
C12:0	0.01	0.01
C14:0	0.04	0.05
C16:0	4.05	4.06
C17:0	0.05	0.04
C18:0	1.82	8.51
C20:0	0.62	0.71
C22:0	0.34	0.35
C24:0	0.15	0.17
Monounsaturated FAME	64.11	83.02
trans-Monounsaturated FAME	0.13	29.93
t-C16:1	0.03	0.16
t-C18:1	0.10	29.30
t-C20:1	0.00	0.42
t-C22:1	0.00	0.00
t-C24:1	0.00	0.04
cis-Monounsaturated FAME	63.97	53.09
c-C16:1	0.21	0.10
c-C18:1	62.32	52.05
c-C20:1	1.26	0.83
c-C22:1	0.03	0.02
c-C24:1	0.16	0.10
Diunsaturated FAME	19.55	2.30
C18:2	19.55	2.30
Triunsaturated FAME	7.77	0.00
C18:3	7.77	0.00
Fuel properties		
Oxidative stability (h)	1.89	38.98
Pour point (°C)	-11	5
Cloud point (°C)	-3	11

6.4.3 Pore Size Effect on TOF

The effect of SiO_2 pore size on the reactivity of the catalyst based on TOF of each C18 FAMEs at a reaction time of 0.5 h is shown in Figure 6.3. The order of the reactivity of each catalyst based on TOF was: Pd/Q3 < Pd/Q10 ~ Pd/Q50 < Pd/Q30. This can be explained from a diffusion limitation of FAMEs into the pores of the SiO_2 support and a contact probability between FAMEs on Pd active site. For Pd/Q3, which is the smallest pore size; bent molecules of C18:3 and C18:2 FAMEs could not penetrate into the small pores (~3 nm). Therefore, it can be suggested that the reaction occurred at Pd active sites located at the outer surface of the SiO_2 support. In addition to the pore size effect, an effect of support acidity was expected to promote the adsorption of FAME molecules on the protonic sites of the SiO_2-Q3 support via interaction between basic unsaturated bonds of unsaturated FAMEs and the Bronsted acid sites. Thus, a weak acidic property of SiO_2-Q3 (Figure 6.1) is another reason for the lowest TOF of the Pd/Q3 catalyst. This acidic property promoted strong adsorption of C18:3 and C18:2 FAMEs on the support with no reaction. However, the TOF of Pd/Q10 was still small when compared with larger pore SiO_2 (Q30). This may be due to the pore diffusion limitation of reactant inside SiO_2-Q10 after the adsorption of liquid FAME molecules on the pore wall. Nevertheless, the TOF of Pd/Q50, which had the biggest pore size, was lower than that of Pd/Q30. The large pore size of SiO_2-Q50 leads to a lesser chance of unsaturated FAME molecules to contact with Pd active sites located inside the SiO_2 pore. According to these results, it can be concluded that pore size of the SiO_2 support has an important effect on the pore diffusion of FAME molecules and contact probability between FAME molecules and Pd active sites.

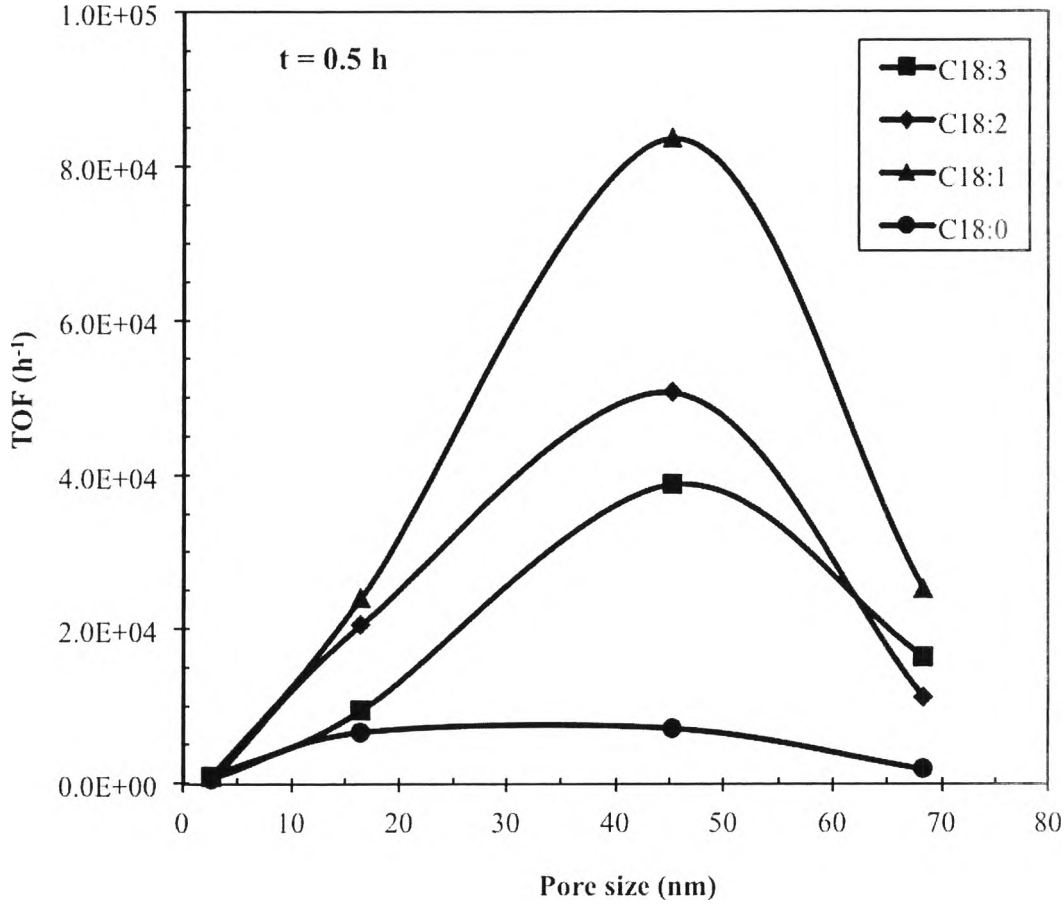

Figure 6.3 Correlation between pore size of the SiO_2 supports and TOF of each C18 FAMEs at 0.5 h of reaction

6.4.4 Pore Size Effect on Selectivity

Furthermore, we also investigated selectivity obtained from using Pd supported on different pore size SiO_2 by comparing at the same depth of hydrogenation (same composition of saturated FAME) as presented in Figure 6.4. It apparently shows a parabolic relationship with an inflection point of the graph at ~23% of saturated FAME. In the first part where the reaction was just beginning (low composition of saturated FAME), the hydrogenation of tri- and diunsaturated to *cis*- and *trans*-monounsaturated FAMEs appeared with a continuously increase of *trans*-monounsaturated FAME (from *cis-trans* isomerization). After that, at the higher composition of saturated FAME, the lower *trans*-monounsaturated FAME composition was observed. This was due to the complete hydrogenation of

monounsaturated to saturated FAME at a longer reaction time. At the same composition of saturated FAME, selectivity towards *trans*-monounsaturated FAME was in this order: Pd/Q10 > Pd/Q30 > Pd/Q50 > Pd/Q3. This was consistent with the result of the pore size effect on TOF, which could be explained in terms of diffusion limitation of FAMEs into the pore of the SiO_2 support and a contact probability between FAMEs on the Pd active sites. The lowest selectivity towards *trans*-monounsaturated FAME of Pd/Q3 was due to the occurring of the reaction outside the pore. Molecules of diunsaturated FAME adsorbed, hydrogenated at the same side, and went out as *cis*-monounsaturated FAME. The reactant had small chance to rotate and adsorb again in another side to generate *trans*-form. In addition, weak acidity of the SiO_2-Q3 could also support this result. It created strong adsorption between basic polyunsaturated FAMEs and its protonic sites. Pd/Q10, where the pore size is bigger than Pd/Q3, therefore the reactant is easily to go inside the pore. Moreover, when compared with Pd/Q30 and Pd/Q50, Pd/Q10 was better fit to the reactant, created a higher possibility of reactant to contact with the active site, and had a longer contact time so there was a higher conversion of original *cis* to *trans*-form during the hydrogenation reaction. However, the pore sizes of SiO_2-Q30 and SiO_2-Q50 were too large, created the low contact probability between the reactant and active site, and consequently, low selectivity towards *trans*-monounsaturated FAME. The presence of *trans*-isomers leads to a much higher melting point than those of the corresponding *cis*-isomers [3]. The melting point of *trans*-C18:1 FAME is 9.9°C, whereas it is only -20.2°C for *cis*-C18:1 FAME [25]. Therefore, *cis*-isomers are preferable in term of cold flow properties point of view. From these results, two possible ways to reduce selectivity towards *trans*-isomers can be suggested: 1) use of non-porous materials as a support as shown in the lowest *trans*-selectivity of Pd/Q3, or 2) use of a large pore size support (macroporous) in order to reduce the contact probability between the reactant and catalyst surface as shown that Pd/Q50 generated low selectivity of *trans*-configuration.

The mechanism of the hydrogenation and isomerization of olefin was described by the work of Horiuti and Polanyi [26]. According to this mechanism, both hydrogenation and isomerization proceed at the same active sites via the half-

hydrogenated intermediates including different stepwise addition and elimination of hydrogen atom.

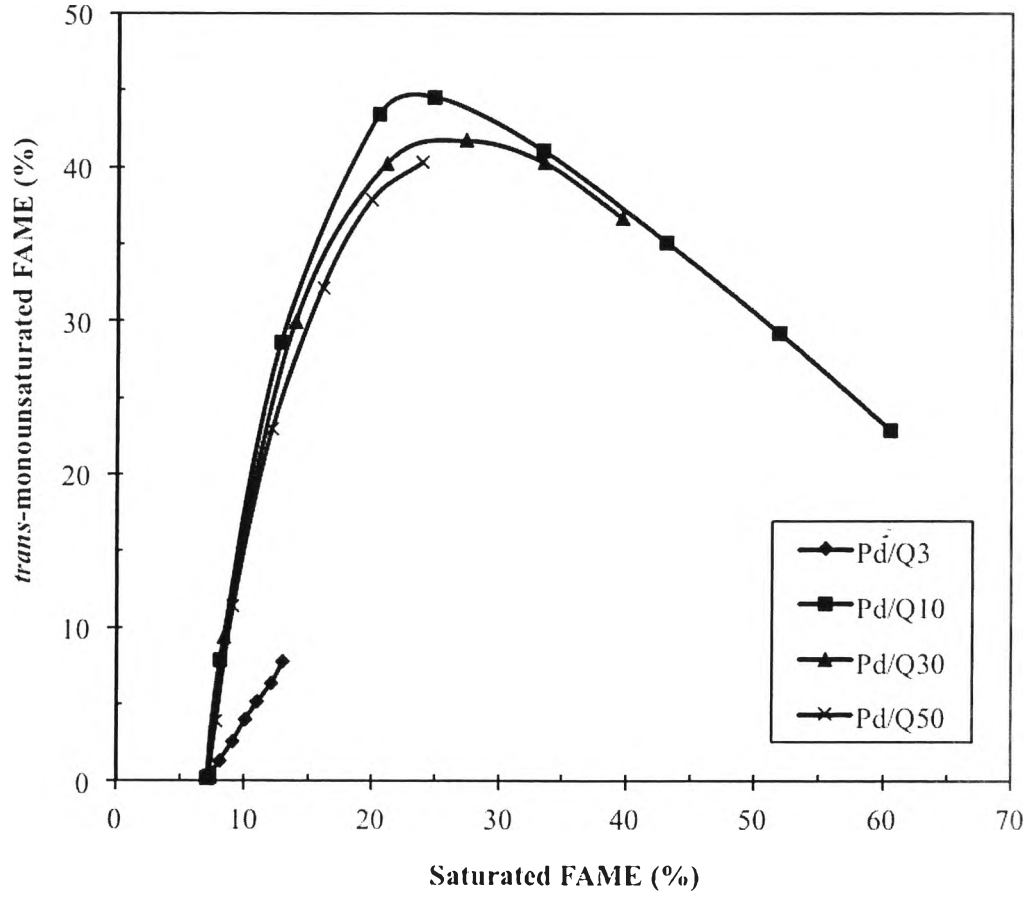

Figure 6.4 Composition of *trans*-monounsaturated FAME as a function of saturated FAME obtained from partial hydrogenation using Pd supported on different pore sizes SiO_2.

6.4.5 Kinetics Analysis

In order to find reaction rate constants for each hydrogenation step of C18 FAMEs; ordinary differential equations of reaction rate were solved by using POLYMATH Professional 6.2, which was supplied from www.polymath-software.com. First, we started with a simple reaction sequence that was proposed by Albright in 1965 [27]. This simple reaction is based on the assumption of the first-

order irreversible reaction. The rate constants: k_1, k_2, and k_3, for this reaction sequence are shown in Equation 6.2.

$$\underset{18:3}{A} \xrightarrow{k_1} \underset{18:2}{B} \xrightarrow{k_2} \underset{18:1}{C} \xrightarrow{k_3} \underset{18:0}{D} \qquad (6.2)$$

The ordinary differential equations of the reaction rate for this reaction sequence were as follows:

$$dA/dt = -k_1A \qquad (6.3(a))$$

$$dB/dt = k_1A - k_2B \qquad (6.3(b))$$

$$dC/dt = k_2B - k_3C \qquad (6.3(c))$$

$$dD/dt = k_3C \qquad (6.3(d))$$

However, this model did not fit well with our experimental data, especially in a period of an increasing of C18:1 and C18:0, as shown in Figure 6.5(A). This may be due to the competitive adsorption of C18:2 and C18:3 on the active Pd site at initiation of the reaction where the concentration of C18:2 and C18:3 is high, so the formation of C18:1 and C18:0 is retarded. After that, we tried to apply a competitive adsorption model to fit the experimental data of C18:1 and C18:0. Here, B; the concentration of C18:2 is a critical variable. If B > 2.5%, Equation 6.3(c) and (d) would be modified to Equation 6.4(a) and (b), respectively.

If B > 2.5%; $dC/dt = k_2B - k_3C^{(1.063-0.0268B)}$ (6.4(a))

If B > 2.5%; $dD/dt = k_3C^{(1.063-0.0268B)}$ (6.4(b))

As presented in Figure 6.5(B), we can see that the competitive adsorption model could fit well with the experimental data. It shows the competitive adsorption of C18:2 with a gradual increase of C18:1 and C18:0 in the initial period of reaction where the concentration of C18:2 was greater than 2.5%. After that, linear decreases and increases of C18:1 and C18:0, respectively, with no competitive adsorption are observed.

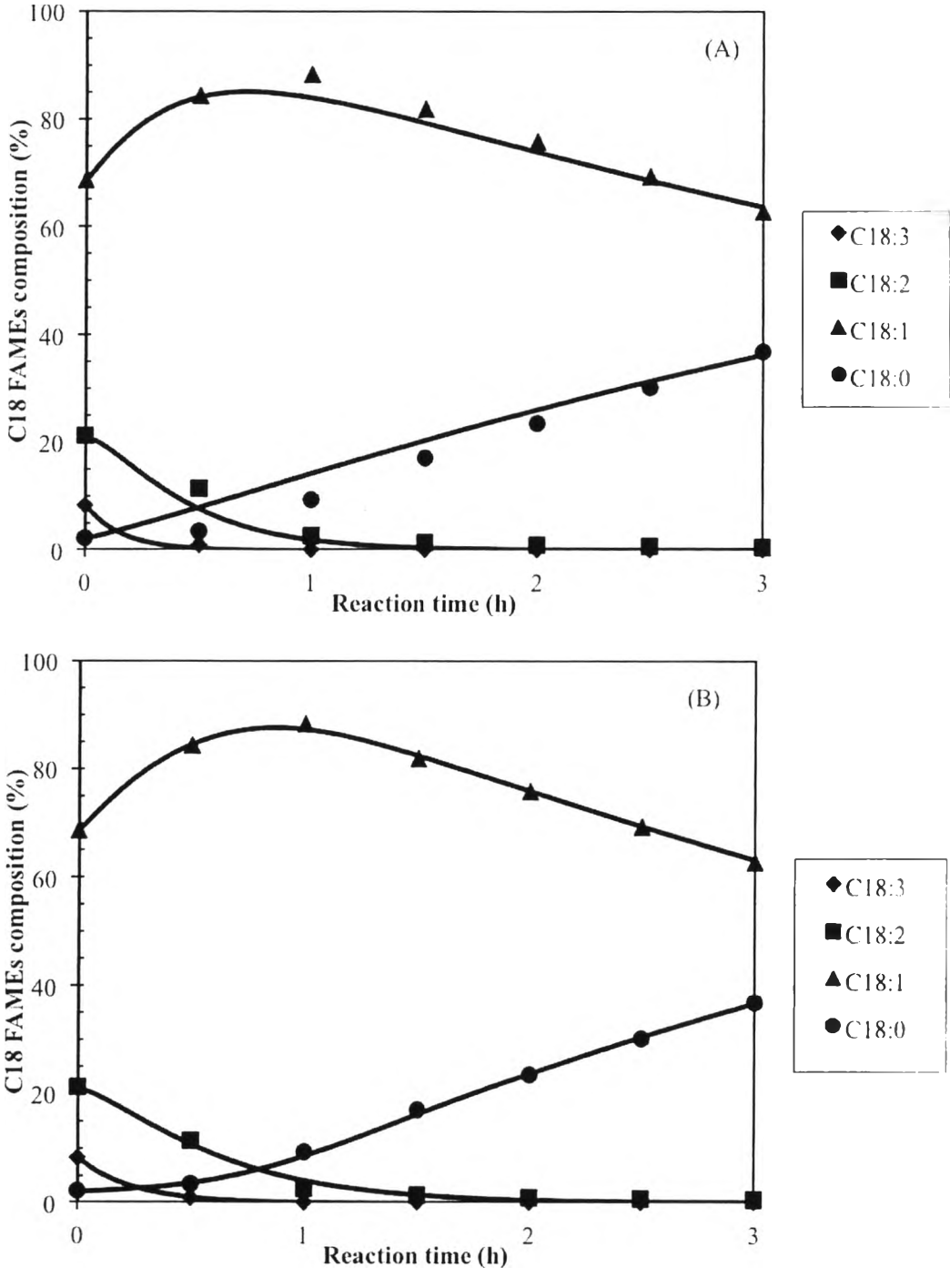

Figure 6.5 Comparison of experimental data (dots) and theoretical estimations from POLYMATH (solid lines) of C18 FAMEs composition as a function of hydrogenation time using Pd/Q30 (A) conventional model and (B) competitive adsorption model

Table 6.3 presents the rate constants and saturation selectivity of Pd supported on different pore sizes SiO_2. *The rate constants are calculated in* unit of $min^{-1}.g_{cat}^{-1}$ and min^{-1}. mole surface $metal^{-1}$. *The latter one is better in* exhibition of a real catalytic activity, which shows the real reaction rate per mole of Pd exposed on the surface. Therefore, we will focus on the rate constants in the *unit of* min^{-1}.mole surface $metal^{-1}$. Saturation selectivity, S_1 and S_2, can be calculated from the ratio of rate constants as shown in Equation 6.5(a) and (b) [28].

$$S_1 = k_1/k_2 \qquad (6.5(a))$$

$$S_2 = k_2/k_3 \qquad (6.5(b))$$

The order of the rate constants of each catalyst were as follows: $k_1 > k_2 > k_3$, and saturation selectivity: S_1 and S_2 were greater than one. These results were consistence with the work done by Allen and co-workers [7]. They investigated the hydrogenation of soybean oil using Ni catalyst and found that k_1 was two times higher than k_2, and k_2 was twelve times higher than k_3. As shown in Table 6.3, we can see that the rate constants of Pd/Q30 are the highest and those of Pd/Q3 are the lowest, which are in the same trend as the effect of pore size on TOF with the reasons of diffusion limitation and contact probability between reactant and active site. When we compare Pd/Q30 and Pd/Q50; we can see that k_1 of Pd/Q30 is almost three times higher than that of Pd/Q50 but their selectivities are not significantly different. This can be explained in terms of higher contact frequency between reactant and active site of the Pd/Q30 catalyst. However, both of them display the same reaction path. When we take into account Pd/Q10, its k_1, k_2, and k_3, are lower than that of Pd/Q30. Moreover, S_1 and S_2 of Pd/Q10 are lowest and highest, respectively, when compared with the other catalysts. Its low S_1 means there is a low hydrogenation tendency from C18:3 to C18:2 because difficulties in pore diffusion of C18:3, but after C18:3 was hydrogenated to C18:2, it could be hydrogenated to C18:1 easily and intern resulted in high k_2. This may be because the ~10 nm pore size SiO_2 fit to the size of C18:2 FAME. On the other hand, Pd/Q3 provided the lowest S_2, about ten times lower than the others, which means very low conversion of C18:2 to C18:1. This can be explained from the low conversion of C18:3 and

C18:2 (low k_1 and k_2), C18:3 and C18:2 strongly adsorbed at the protonic sites of the Q3 support without any reaction. These results confirm the suggestion of selectivity towards *trans*-monounsaturated FAME (Figure 5.4).

Table 6.3 Rate constants and saturation selectivities of Pd supported on different pore sizes SiO_2.

Catalyst	Rate constant						Saturation selectivity	
	k_1	k_2	k_3	k_1	k_2	k_3		
	(min^{-1}.g catalyst^{-1})			($x10^2$ min^{-1}.mol surface metal^{-1})			S_1	S_2
Pd/Q3	0.032	0.015	0.010	7.1	3.4	2.2	2.09	1.54
Pd/Q10	0.328	0.278	0.017	115.2	97.6	5.9	1.18	16.67
Pd/Q30	0.222	0.122	0.011	360.9	198.5	17.1	1.82	11.64
Pd/Q50	0.150	0.067	0.006	137.0	60.9	5.8	2.25	10.43
Ni[(a)]	0.367	0.159	0.013	-	-	-	2.31	12.23

[(a)]Hydrogenation of soybean oil at 175°C, 0.1 MPa, 600 rpm using 0.02% Ni catalyst [7]

6.4.6 Pore Size Effect on Fuel Properties of Hydrogenated FAMEs

The oxidative stability of hydrogenated FAMEs obtained from using Pd supported on different pore size of SiO_2 was investigated. Figure 6.6(A) shows the composition of polyunsaturated FAMEs (C18:2 and C18:3) as a function of oxidative stability. After hydrogenation; the composition of C18:2 and C18:3 decreased with an improvement of oxidative stability. The longer hydrogenation time, the lower composition of C18:2 and C18:3, and the higher oxidative stability

are observed for all catalysts. It apparently shows that SiO_2 pore size has an effect on oxidative stability, especially in the range of 1% to 9% of C18:2 and C18:3 composition. In this range, the oxidative stability of hydrogenated BDF products were in this order: Pd/Q30 > Pd/Q10 > Pd/Q50. This order of the oxidative stability was due to the different in C18:3 composition. As shown in Table 6.4, only 0.01% different in composition of C18:3, a big different in the oxidative stability was observed. Relative oxidation rate of C18:3, C18:2, and C18:1 FAMEs are 98, 41, and 1, respectively [29]. This means C18:3 can be oxidized about two times more easily than C18:2 and almost hundred times than C18:1. Therefore, C18:3 is an important parameter that determine the oxidative stability of biodiesel, i.e., the hydrogenated BDF of Pd/Q50, which contains higher amount of C18:3, presents the lower oxidative stability when compared with Pd/Q10 and Pd/Q30. On the other hand, Pd/Q3, which shows the lowest hydrogenation activity, contained the highest composition of C18:2 and C18:3 and resulted in the lowest oxidative stability, which could not pass Thai standards (requires $\geq$ 10 h).

Table 6.4 Comparison of C18 FAMEs composition and fuel properties at a similar point of C18:2 and C18:3 composition shown in Figure 6.6(A).

Catalyst	C18:2+C18:3 (%)	C18:3 (%)	C18:2 (%)	C18:1 (%)	C18:0 (%)	Oxidative stability (h)	Cloud point (^{o}C)
Pd/Q10	2.91	0.01	2.90	81.97	7.43	25.63	10
Pd/Q30	2.30	0.00	2.30	81.35	8.51	38.98	11
Pd/Q50	2.26	0.02	2.24	79.10	10.59	13.70	12

Moreover, the cloud point of biodiesel product was investigated as presented in Figure 6.6(B). Here, the cloud point of hydrogenated FAMEs was considered along with composition of C18:0, which is the main components of saturated FAMEs in the rapeseed BDF. With a higher degree of hydrogenation (longer reaction time), the greater amount of C18:0, results in an increasing of cloud

point. It shows that the effect of SiO_2 pore size on cloud point does not appear apparently. Nevertheless, it obviously shows a point of inflection at ~9% of C18:0. As can be seen in Figure 6.6(B); a rapid increase of cloud point is observed initially and then, at ~9% of C18:0; a slow increase of cloud point is observed. However, this inflection point was not at the same position (same composition of saturated FAME) as the relationship between *trans*-monounsaturated and saturated FAME (Figure 6.4), which shows an inflection point of parabolic graph at ~23% of saturated FAME, even though, C18:0 is the main component in the saturated FAME. This suggested that the cloud point does not only relate to the formation of C18:0 and *trans*-C18:1 but also combining the formation of total saturated FAMEs, especially C16:0, which has a high melting point (28.5°C) [25]. Initially, small amount of C16:0, C18:0, and other saturated FAMEs were formed, leaded to an appearance of small crystals that were easy to freeze, with a rapidly increase of cloud point. After that, a lot of crystal deposited and resulted in slowly increase of the cloud point. Thus, total saturated FAMEs composition and formation of *trans*-monounsaturated FAME would be important parameters to determine the cold flow properties of biodiesel.

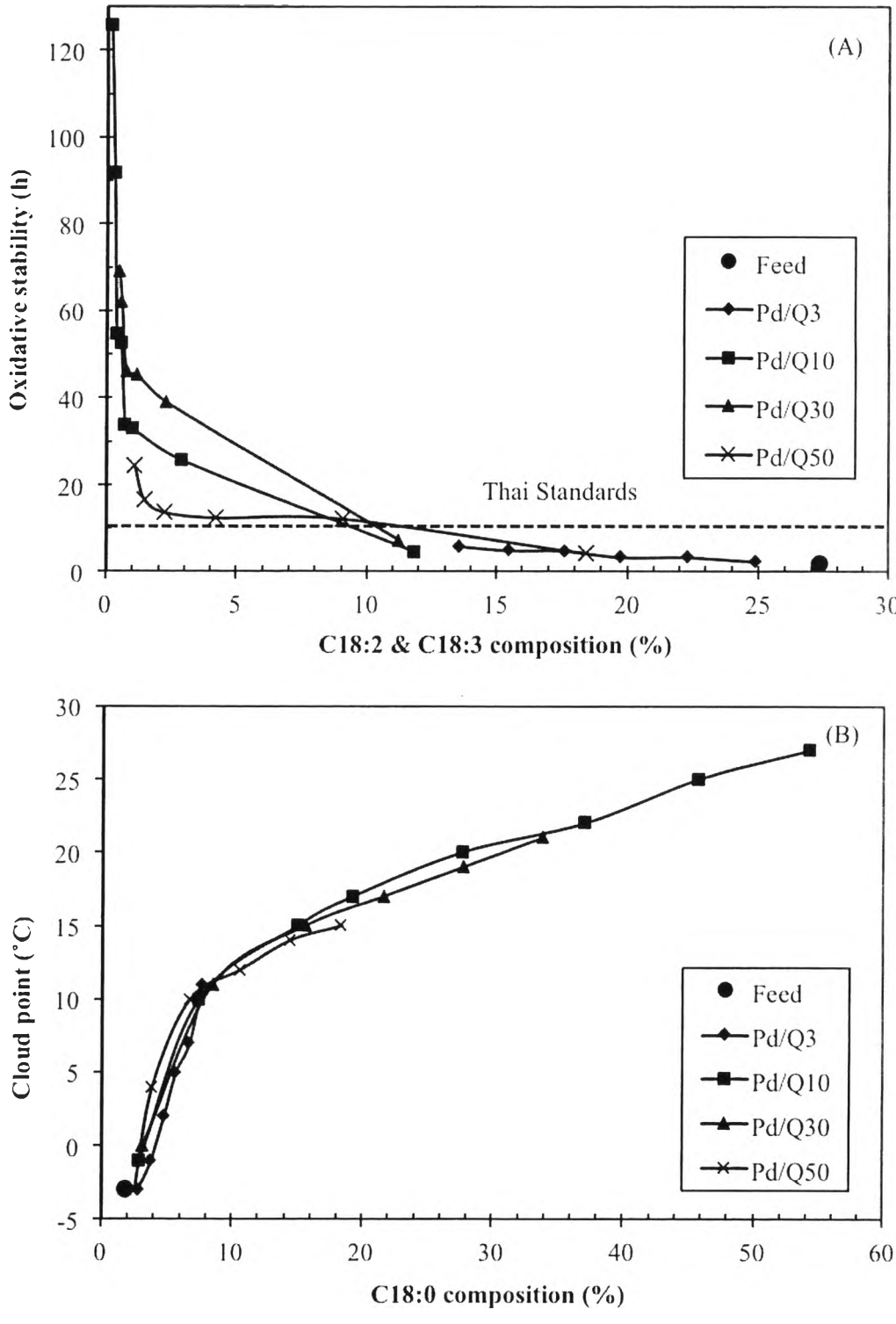

Figure 6.6 Oxidative stability (A) and cloud point (B) of BDF feed and products after hydrogenation using Pd supported on different pore sizes SiO_2.

6.5 Conclusions

Partial hydrogenation of polyunsaturated FAMEs of rapeseed biodiesel has been investigated on Pd/SiO_2 catalysts. It was found that these catalysts provided good partial hydrogenation activity, resulting in an improvement of oxidative stability. Moreover, it can be concluded that the pore size of the SiO_2 support had a significant effect on the activity of the catalyst. The pore size affected pore diffusion of the reactants and contact probability between the reactants and Pd active sites. Hydrogenation activity studied in terms of turn over frequency (TOF) and reaction rate constants (k_1, k_2, and k_3), shows that Pd on ~45 nm (Q30) pore size SiO_2 exhibits the highest hydrogenation activity. Furthermore, the *cis-trans* selectivity depends on contact probability between reactant and catalyst. The selectivity towards *cis*-monounsaturated FAME was found to be high for Pd on ~2 nm (Q3) and ~68 nm (Q50) pore size SiO_2 due to the low contact probability between FAME molecules and active sites in very small and large pores. Despite from the small pore size of SiO_2-Q3, the adsorption of FAME molecules on its protonic sites also promoted high *cis*-selectivity. Therefore, two possible ways to reduce selectivity towards *trans*-isomers can be suggested: 1) use of non-porous materials as a support or 2) use of a large pore size support (macroporous) in order to reduce the contact probability between the reactant and catalyst surface.

6.6 Acknowledgements

The authors would like to thank the Chulalongkorn University Dutsadi Phipat Endowment Fund, Chulalongkorn University, Thailand and the Center of Excellence on Petrochemicals and Materials Technology, Thailand, for their financial support. And deeply thanks to Dr. Takehisa Mochizuki and Ms. Yohko Abe, National Institute of Advanced Industrial Science and Technology, Japan for their helps on instrumental analysis.

6.7 References

[1] I.N. Martyanov, A. Sayari, Appl. Catal. A: Gen. 339 (2008) 45–52.

[2] Z. Helwani, M.R. Othman, N. Aziz, J. Kim, W.J.N. Fernando, Appl. Catal. A: Gen. 363 (2009) 1–10.

[3] G. Knothe, Energy Fuels 22 (2008) 1358–1364.

[4] T. Sonthisawate, A. Suemanotham, Y. Yoshimura, T. Makoto, Y. Abe, Global Warming Conference: Biodiversity and Their Sustainable Use, 2009, pp. 90–97.

[5] C.E. Papadopoulos, A. Lazaridou, A. Koutsoumba, N. Kokkinos, A. Christoforidis, N. Nikolaou, Bioresour. Technol. 101 (2010) 1812–1819.

[6] H.W.B. Patterson, in: G.R. List, J.W. King (Eds.), Hydrogenation of Fats and Oils: Theory and Practice, second ed., American Oil Chemist's Society Press, 2011, pp. 169–187.

[7] R.R. Allen, M.W. Formo, R.G. Krishnamurthy, G.N. McDermott, F.A. Norris, N.O.V. Sonntag, in: D. Swern (Ed.), Bailey's Industrial Oil and Fat Products, fourth ed., A Wiley-Interscience Publication, John Wiley & Sons, 1982, pp. 1–95.

[8] M. Zajcew, J. Am. Oil Chem. Soc. 37 (1960) 130–132.

[9] P.N. Rylander, Hydrogenation Methods, Academic Press, New York, 1985.

[10] G. Hoffmann, The Chemistry and Technology of Edible Oils and Fats and Their High Fat Products, Academic Press, 1989.

[11] T. Harada, S. Ikeda, M. Miyazaki, T. Sakata, H. Mori, M. Matsumura, J. Mol. Catal. A: Chem. 268 (2007) 59–64.

[12] H. Tamai, U. Nobuaki, H. Yasuda, Mater. Chem. Phys. 114 (2009) 10–13.

[13] K. Wadumesthrige, S.O. Salley, K.Y.S. Ng, Fuel Process. Technol. 90 (2009) 1292–1299.

[14] J.C. Rodríguez, J. Santamaría, A. Monzon, Appl. Catal. A: Gen. 165 (1997) 147–157.

[15] I.Y. Ahn, J.H. Lee, S.K. Kim, S.H. Moon, Appl. Catal. A: Gen. 360 (2009) 38–42.

[16] S.D. Jackson, A. Monaghan, Catal. Today 128 (2007) 47–51.

[17] K. Pattamakomsan, E. Ehret, F. Morfin, P. Gélin, Y. Jugnet, S. Prakash, J.C. Bertolini, J. Panpranot, F. Jose Cadete Santos Aires, Catal. Today 164 (2011) 28–33.

[18] A.D. Schmitz, G. Bowers, C. Song, Catal. Today 31 (1996) 45–56.

[19] W. Huang, W. Pyrz, R.F. Lobo, J.G. Chen, Appl. Catal. A: Gen. 333 (2007) 254–263.

[20] J. Panpranot, K. Pattamakomsan, J.G. Goodwin Jr., P. Praserthdam, Catal. Commun. 5 (2004) 583–590.

[21] H. Li, J. Liu, H. Yang, H. Li, Chin. J. Chem. 27 (2009) 2316–2322.

[22] M.J. Ramos, C.M. Fernandez, A. Casas, L. Rodríguez, A. Pérez, Bioresour Technol. 100 (2009) 261–268.

[23] A.F. Pérez-Cadenas, M.M.P. Zieverink, F. Kapteijn, J.A. Moulijn, Catal. Today 105 (2005) 623–628.

[24] S. Goto, M. Oguma, N. Chollacoop, L. Dowling, D. Sheedy, W. Zhang, et al., EASERIA Biodiesel Fuel Trade Handbook: 2010, Economic Research Institute for Asian and East Asia (ERIA), Jakarta, 2008 (1st printed).

[25] G. Knothe, R.O. Dunn, J. Am. Oil Chem. Soc. 86 (2009) 843–856.

[26] I. Horiuti, M. Polanyi, Trans. Faraday Soc. 30 (1934) 1164–1172.

[27] L.F. Albright, J. Am. Oil Chem. Soc. 42 (1965) 250–253.

[28] M. Naglic, A. Smidovnik, T. Koloini, J. Am. Oil Chem. Soc. 75 (1998) 629–633.

[29] E.N. Frankel, Lipid Oxidation, The Oily Press, Dundee, Scotland, 1998.